© 2018. Published by The Company of Biologists Ltd | Journal of Experimental Biology (2018) 221, jeb177758. doi:10.1242/jeb.177758

RESEARCH ARTICLE

Locomotor muscle fibre heterogeneity and metabolism in the fastest large-bodied rorqual: the fin whale (*Balaenoptera physalus*)

José-Luis L. Rivero*

ABSTRACT

From a terrestrial ancestry, the fin whale (*Balaenoptera physalus*) is one of the largest animals on Earth with a sprinter anti-predator strategy, and a characteristic feeding mode, lunge feeding, which involves bouts of high-intensity muscle activity demanding high metabolic output. We investigated the locomotor muscle morphology and metabolism of this cetacean to determine whether its muscle profile (1) explains this unique swimming performance and feeding behaviour, (2) is or is not homogeneous within the muscle, and (3) predicts allometric variations inherent to an extreme body size. A predominantly fast-glycolytic phenotype characterized the fin whale locomotor muscle, composed of abundant fast-twitch (type IIA) fibres with high glycolytic potential, low oxidative capacity, relatively small size, and reduced number of capillaries. Compared with superficial areas, deep regions of this muscle exhibited a slower and more oxidative profile, suggesting a division of labour between muscle strata. As expected, the fin whale locomotor muscle only expressed the two slowest myosin heavy chain isoforms (I and IIA). However, it displayed anaerobic (glycolytic) and aerobic (lipid-based metabolism) capabilities higher than would be predicted from the allometric perspective of its extreme body size. Relationships between muscle metabolism and body mass were fibre-type specific. The 'sprinter' profile of the fin whale swimming muscle, particularly of its superficial compartment, supports physiological demands during both high-speed swimming and the lunge, when energy expenditure reaches maximal or supramaximal levels. Comparatively, the slower and more oxidative profile of the deep compartment of this muscle seems to be well designed for sustained, low-intensity muscle activity during routine swimming.

KEY WORDS: Skeletal muscle, Muscle fibre types, Muscle metabolism, Marine mammals, Cetacean, Aerobic dive limit

INTRODUCTION

The morphology and physiology of a marine mammal's skeletal muscle provides insight into its aerobic dive limit (ADL) and diving behaviour (Kanatous et al., 2002; Williams and Noren, 2011; Kielhorn et al., 2013; Velten et al., 2013). Marine mammals that perform deep, long-duration dives share muscle features that contribute to extending their ADLs when compared with short-duration, shallow-diving species. These muscle adaptations include elevated myoglobin (Mb) concentrations and a muscle phenotype composed of larger and abundant slow-oxidative (type I) fibres with lower mitochondrial volume densities (V_{mt}) in deep- versus shallow-diving species (Kanatous et al., 2002; Polasek et al., 2006; Williams and Noren, 2011; Kielhorn et al., 2013). By staying within its ADL, a diving mammal increases its foraging efficiency by decreasing the time it must spend at the surface metabolizing the lactate resulting from anaerobic metabolism (Kooyman et al., 1980). However, tagging (Tyack et al., 2006) and morphological muscle (Velten et al., 2013) studies of extreme diving cetaceans have challenged the view that most marine mammals dive aerobically. These studies suggest that, at low metabolic rates, these cetaceans perform their dives aerobically within their calculated ADLs, but at high metabolic rates, they can perform dives anaerobically that are likely to exceed their calculated ADLs (Velten et al., 2013).

The large rorqual species, of which fin whales (*Balaenoptera physalus*) are members, are a family of exceptionally streamlined baleen whales (mysticetes) that were secondarily adapted to marine environments from a terrestrial ancestry (Marx et al., 2016). These species exhibit a type of ram-feeding strategy (lunge-feeding) that is considered the largest biomechanical event on Earth (Brodie, 1993). During engulfment, massive amounts of prey and water are engulfed and filtered intermittently either at the sea surface or multiple times during a foraging dive (Goldbogen et al., 2006). This feeding strategy, which needs dynamic water pressure, or in other words drag, demands well-coordinated actions of the buccal cavity and locomotor muscles (Potvin et al., 2009).

Rorquals usually dive to shallower depths and for shorter periods (Croll et al., 2001) than would be predicted from an allometric consideration of their extreme body size (Halsey et al., 2006). The purported high energetic cost of lunge-feeding is currently thought to be the proximate cause of this limited diving capacity (Croll et al., 2001; Goldbogen et al., 2008). A recent study has revealed that the engulfment metabolism increases across the full body size of the larger rorqual species to nearly 30–40 times the basal metabolic rate of terrestrial mammals of comparable body mass (Potvin et al., 2012). Moreover, it was suggested that the metabolism of the largest body sizes runs with significant oxygen deficits during mouth opening, namely, 20% over the maximum aerobic capacity at the size of the largest whales, thus requiring significant contributions from anaerobic catabolism during a lunge (Potvin et al., 2012).

Beyond this impressive feeding mode, the ability of fin whales and other *Balaenoptera* whales to swim at relatively high speeds for a long time is well documented (Ford and Reeves, 2008). During routine activities, such as foraging and migration, these species usually swim at speeds <10 km h^{-1} (Watkins et al., 1996; Tyack et al., 2006). Possibly as a result of predation pressure, *Balaenoptera* whales have developed a strategy that consists of rapid

Laboratory of Muscular Biopathology, Department of Comparative Anatomy and Pathological Anatomy, Faculty of Veterinary Sciences, University of Cordoba, Campus Universitario de Rabanales, 14014 Cordoba, Spain.

*Author for correspondence (an1lorij@uco.es)

J.-L.L.R., 0000-0001-7706-609X

Received 19 January 2018; Accepted 18 April 2018

Journal of Experimental Biology (2018) 221, jeb177758. doi:10.1242/jeb.177758

List of abbreviations

ADL	aerobic dive limit
CS	citrate synthase
CSA	cross-sectional area
GPDH	glycerol-3-phosphate dehydrogenase
HAD	β-hydroxyacyl coenzyme A dehydrogenase
LDH	lactate dehydrogenase
MAb	monoclonal antibody
mATPase	myofibrillar adenosine triphosphatase
Mb	myoglobin
MG-1	anti-myoglobin monoclonal antibody
MHC	myosin heavy chain
MMR	maximum metabolic rate
OD	optical density
ORO	oil red O
PAS	periodic acid Schiff
RMR	resting metabolic rate
SDH	succinate dehydrogenase
VGB	ventral groove blubber
V_{mt}	mitochondrial volume density

(20–40 km h^{-1}) directional swimming away from predators (Ford and Reeves, 2008). Fin whales, with a recorded top speed of up to 50 km h^{-1} (Tomilin, 1957), are considered the fastest among the rorqual whales (Ford and Reeves, 2008). They can sustain efficient propulsion at speeds of 21–29 km h^{-1} which allows them sufficient time to outpace pursuing predators (Bose and Lien, 1989). In addition to their morphological adaptations to speed, which favour their hydrodynamic properties as in other large rorquals of the same genus (Ford and Reeves, 2008), fin whales can achieve swim speeds greater than other whales, probably because its propulsive muscle mass adapts well to this task.

To our knowledge, only Mb content has been assessed in baleen whales (Noren and Williams, 2000), but comprehensive data on locomotor muscle morphology and metabolism are not available for these cetaceans.

In marine mammals, some studies have revealed that muscle fibre types (Dearolf et al., 2000), [Mb] (Polasek and Davis, 2001) and V_{mt} (Watson et al., 2007) are not homogeneously distributed within epaxial muscles in several cetacean and pinniped species, suggesting a division of labour between different subvolumes of the epaxial musculature. As baleen whales exhibit differential diving behaviour between foraging (Croll et al., 2001) and non-foraging dives (Ford and Reeves, 2008), one might expect their epaxial muscles to display structural and functional specializations as part of their fascinating process of adaptation to marine environments from a terrestrial ancestry (Marx et al., 2016). The short bouts of high-intensity muscle activity with extremely high metabolic output that demand the extreme body size and the bulk-filter feeding mode of the fin whale, as well as its sustained high-speed swimming used as an anti-predator strategy, must be correlated with a fast-glycolytic skeletal muscle phenotype. In contrast, the sustained, low-intensity muscle activity involved in non-feeding travel must be related to a comparatively slower and more oxidative muscle phenotype.

The skeletal muscle profile of rorquals is also interesting from an allometric perspective, as body mass plays a principal role in determining contractile and metabolic features of mammalian muscle fibres (Schiaffino and Reggiani, 2011). A relationship between myosin heavy chain (MHC) expression, the most useful marker of fibre types, and body size is well known in terrestrial mammals (Schiaffino and Reggiani, 2011). Immunohistochemical (Watson et al., 2003) and electrophoretic (Dearolf, 2003) studies have shown that adult marine mammals only express one slow (type I)- and one fast (presumably type IIA)-contracting MHC, but identities of these MHC isoforms have not been accurately characterized. Body size is also relevant for energy metabolism (Weibel and Hoppeler, 2005). Several studies have shown a significant relationship between muscle V_{mt} and body mass in a variety of terrestrial and marine mammals varying largely in body size (Kanatous et al., 2002; Watson et al., 2007; Velten et al., 2013). However, these estimations have assumed that the two main fibre types of marine mammals have similar oxidative capabilities (Kanatous et al., 2002; Watson et al., 2007). Recent studies in cetaceans indicate that both total V_{mt} (Velten et al., 2013) and histochemical succinate dehydrogenase (SDH) activity, used as an indirect index of mitochondrial density (Kielhorn et al., 2013), are significantly higher in type I than in type II muscle fibres. Thus, it is reasonable to hypothesize that the relationship between muscle metabolism and body mass could be fibre-type specific.

The present study examines fibre-type characteristics (proportion, metabolic profiles, Mb content, size and capillarization) and whole-muscle metabolic indicators [lactate dehydrogenase (LDH), citrate synthase (CS) and β-hydroxyacyl coenzyme A dehydrogenase (HAD) enzyme activities, and Mb content] in the primary locomotor longissimus dorsi muscle of the fin whale. The main objective was to gain insight into the relationship between locomotor muscle characteristics and both swimming and feeding behaviours of this species. It was expected that the locomotor muscle of this large cetacean would display the characteristic fast-glycolytic design that accompanies fast swimmers. A second goal was to test whether the locomotor longissimus muscle of the fin whale is homogeneous across different depths and cranio-caudal locations. It was hypothesized that a division of labour between different muscle subvolumes should be reflected by relevant regional variations in fibre-type proportions and metabolic indicators. Finally, a third aim of the present study was to contribute to our understanding of the role that body size plays in determining contractile and metabolic features of mammalian skeletal muscle fibre types. It was expected that the locomotor muscle of the fin whale expresses only the slowest-contracting MHC isoforms (i.e. MHCs I and IIA) with complete absence of the fast-contracting IIX and IIB MHC isoforms. Based on allometric trends of decreased muscle aerobic capacity and increased muscle anaerobic capacity that accompany larger body sizes (Emmett and Hochachka, 1981; Kanatous et al., 2002; Velten et al., 2013), it was also hypothesized that there would be a decreased oxidative capacity and an enhanced glycolytic potential in locomotor muscle fibre types of the fin whale.

MATERIALS AND METHODS

Specimens and muscle sampling collection

This study utilized an archive of frozen muscle samples removed from four fin whales that were found stranded along the Mediterranean coast (three cases) or on the Spanish northwest Atlantic coast (one case) between September 2004 and January 2011. The animals were of both sexes (two males and two females) and ranged in age from juvenile (one male 6 m in length and an estimated mass of ∼2600 kg; and one female 7.8 m in length and an estimated mass of ∼5000 kg) to subadult (one female 12.7 m in length and an estimated mass of ∼15,500 kg) or adult (one male 16.1 m in length and an estimated mass of ∼25,000 kg) according to biological and morphometric features (Boyd et al., 1999). All specimens were of high quality and scored either Code 1 (alive at the time of stranding and died or euthanized; two cases) or Code 2

Journal of Experimental Biology (2018) 221, jeb177758. doi:10.1242/jeb.177758

(freshly dead; two cases) according to rules of the Smithsonian Institution (Geraci and Lounsbury, 2005). A detailed post-mortem examination within 24 h after stranding was performed either *in situ* (three cases) or in the necropsy room at the Veterinary School of Cordoba, Spain (one case). No actuations were performed on live animals.

In all four specimens, samples of the primary locomotor muscle longissimus dorsi were collected within 24–36 h of the animal's stranding date following a standardized muscle sampling protocol (see below). This muscle works to power the dorsal/ventral spinal flexion that generates thrust through the tail flukes during swimming (Polasek and Davis, 2001). Five samples per muscle area were taken either unilaterally (three animals) or bilaterally (one juvenile case) in four different areas of the muscle to test the potential heterogeneity of fibre-type characteristics and metabolic markers. They corresponded to two superficial (just ventral to the superficial tendon located under the dorsal blubber) and two deep (lying closest to the vertebrae) areas situated at the middle (just at the position of the dorsal fin) and at the caudal (lower lumbar area, half-way between dorsal fin and fluke) regions of the muscle.

After collection, muscle samples weighing 100–150 mg were placed in cooled, airtight containers on ice until frozen within 6–8 h. One half of the sample, designated for fibre-typing morphology, was frozen in isopentane (30 s), kept at the freezing point in liquid nitrogen, and the other half of the sample was directly quenched in liquid nitrogen, stored at −80°C, and used for biochemical analysis.

Characterization of myosin heavy chain isoforms

To characterize MHC isoforms expressed in fin whale skeletal muscle, MHC electrophoresis (8% SDS-PAGE) and immunoblot analyses [nitrocellulose filters stained with monoclonal antibodies (MAb)] were performed following the protocols described in detail by Talmadge and Roy (1993) and Rossini et al. (1995), respectively. A battery of five MAbs specific for the four mature MHC isoforms identified as types I, IIA, IIX and IIB (see Table 1 for specificities and sources of these MAbs) was used for the accurate identification of electrophoretic MHC bands, as previously described (Acevedo and Rivero, 2006). Once these isoforms were identified (see Results section), electrophoretic gels were scanned and quantification of each MHC isoform was obtained in relative terms of each muscle sample as previously detailed (Rivero et al., 1997).

Table 1. Immunochemical characterization of fin whale muscle fibre types

	Specificity for rat MHC isoforms			
MAbs	I	IIA	IIX	IIB
BA-F8	+	–	–	–
SC-75	–	+	+	+
SC-71	–	+	+	–
BF-35	+	+	–	+
S5-8H2	+	–	+	+

	Fin whale muscle fibre types or MHC isoform		
MAbs	I	I+IIA	IIA
BA-F8	+	+	–
SC-75	–	+	+
SC-71	–	+	+
BF-35	+	+	+
S5-8H2	+	+	–

Specificity of monoclonal antibodies (MAbs) used in the study against rat myosin heavy chain (MHC) isoforms according to Schiaffino et al. (1989) (clones BA-F8, SC-75, SC-71 and BF-35) and Rivero et al. (1999) (clone S5-8H2). Immunohistochemical MHC-based fibre-types of the longissimus muscle of fin whales (*B. physalus*) are delineated as either positive (+) or negative (–) immunostaining for a specific fibre-type with that MAb. Fibre-types I and IIA are pure phenotypes expressing a unique MHC isoform (MHC-I and MCH-IIA, respectively); I+IIA are hybrid fibres with co-expression of MHCs I and IIA. Sources of these MAbs: DMS, Braunchweig, Germany (clones BA-F8, SC-75, SC-71 and BF-35) and Biocitex Biotechnology, Marseille, France (MAb S5-8H2).

Characterization of muscle fibre types

To investigate their involvement in muscle function, a full, comprehensive and quantitative characterization of the fibre-type composition, including contractile, metabolic and morphological features of the fin whale muscle fibre types, was made by combined methodologies of immunohistochemistry, quantitative histochemistry and image analysis (Quiroz-Rothe and Rivero, 2004; Acevedo and Rivero, 2006).

Briefly, frozen samples were cross-sectioned serially in a cryostat and were used for immunohistochemistry and quantitative histochemistry. Serial sections were reacted with a panel of MHC isoform-specific MAbs (Table 1) following the immunoperoxidase protocol described by Rivero et al. (1996b). An additional serial section reacted with an anti-Mb MAb produced in mouse (clone MG-1, code M773; Sigma-Aldrich, USA), and used to quantify the Mb content of individual fibres as described below.

Additional serial sections were stained for myofibrillar adenosine triphosphatase (mATPase) histochemical activity after acid (pH 4.4., 2 min) and alkaline (pH 10.5, 10 min) pre-incubations using a modification (Nwoye et al., 1982) of the Brooke and Kaiser (1970) method for the acid pre-treatment, and of the Guth and Samaha (1969) method for the alkaline pre-incubation. The histochemical activity of the succinate dehydrogenase (SDH, EC 1.3.5.1), an enzyme located on the inner mitochondrial membrane used as an oxidative marker, and the glycerol-3-phosphate dehydrogenase (GPDH, EC 1.1.1.8), a cytosolic enzyme used as a glycolytic indicator, were determined according to the quantitative procedures described by Blanco et al. (1988) and Martin et al. (1985), respectively, except that the thick sections for GPDH staining were 14 µm and the optimum incubation times were 10 min for the SDH and 30 min for the GPDH. These muscle enzyme activities were expressed as steady-state rates in optimal densities (OD) min^{-1}. Additional serial sections of the same muscle samples were stained for periodic acid Schiff (PAS, used to quantify relative glycogen content of muscle fibres), oil red O (ORO, for visualizing intracellular lipid droplets), PAS followed by digestion with α-amylase (for visualizing capillaries), and haematoxylin eosin (used to visualize morphology of muscle fibres) according to standardized protocols described previously (Dubowitz and Sewry, 2007).

Sections were visualized with a microscope connected to a high-resolution device-camera and a computer equipped with a frame-grabber and image-analysing software as previously detailed (Acevedo and Rivero, 2006). An area containing ∼150 fibres was digitized in all sections (Acevedo and Rivero, 2006). A mean OD of the same single fibres included in the selected muscle area was derived in either duplicate (immunohistochemistry, mATPase histochemistry, PAS, ORO and MG-1) or triplicate (SDH and GPDH reactions) serial sections for each staining. Staining intensities were expressed as end-point ODs for mATPase, PAS, ORO and MG-1 stains. The cross-sectional area (CSA, $µm^2$) and the mean number of capillaries [expressed in absolute and relative terms (as number of capillaries per 1000 $µm^2$ of the fibre CSA)] of the same individual fibres were also determined on the α-amylase PAS stain.

The muscle fibres included in the selected area of each muscle sample were typified according to their MHC content judged

visually by immunohistochemistry, and the proportion of muscle fibre types was calculated for each muscle sample (for details, see Acevedo and Rivero, 2006). To estimate the potential correlation between the immunohistochemical MHC content and the histochemical mATPase activity of fin whale muscle fibre types, the muscle fibre-type composition of each muscle sample was also derived from a combined inspection of both acid and alkaline mATPase pre-incubations as previously detailed (Rivero et al., 1996a). Quantitative information obtained for each muscle sample (OD, CSA and capillaries) was averaged according to MHC-based fibre types and used for statistical analyses.

Metabolic indicators and Mb content

The activities of the enzymes LDH (EC 1.1.1.27), CS (EC 4.1.3.7) and HAD (EC 1.1.1.35) were measured in duplicate for each sample as previously described (Rivero et al., 1995). The activity of each muscle enzyme was calculated in units of μmol NADH converted per minute per gram of freeze-dried muscle. Enzyme activity ratios (LDH/CS, CS/HAD) were calculated to assess the relative contribution of different metabolic pathways in the muscle (Polasek et al., 2006).

The method of Reynafarje (1963) was used to determine Mb concentration. Briefly, aliquots from the same supernatants used for muscle enzyme assays were diluted with phosphate buffer (0.04 mmol l^{-1}, pH 6.6), and the resulting mixture was centrifuged for 50 min at 28,000 ***g*** at 4°C. The supernatant was bubbled with 99.9% carbon monoxide for 5 min to convert the Mb to carboxymyoglobin. After bubbling, the absorbance of the supernatant at 538 and 568 nm was measured using a Bio-Tek PowerWave 340X microplate reader. A Mb standard (horse Mb, Sigma-Aldrich, USA) was run with each set of samples, and the Mb concentration was calculated as described by Reynafarje (1963) and expressed in mg per gram of wet tissue mass.

Statistical analyses

All statistics and charts were run in Statistica 7.0 for Windows (StatSoft I; www.statsoft.com). Data obtained for the five samples examined in each muscle sampling area were averaged and mean values were used in further analyses (Table S1). Sample size and the power of a contrast of hypotheses were estimated by power analysis and interval estimation. In general, accepting an α-risk of 0.05 and a β-risk of 0.02 in a two-sided test, a minimum of 10 samples (two independent samples per animal) per each comparison was necessary to recognize as statistically significant a difference greater than 1 times the standard deviation between comparisons, assuming a common deviation of 20% of the mean values and anticipating a drop-out rate of 0%. Normality of muscle variables was tested using a Kolmogorov–Smirnov test, and data were expressed as means±s.e.m. Two-tailed Student's paired *t*-test for dependent samples was used to test for differences between muscle locations (middle versus caudal region of the muscle), between sampling depths (superficial versus deep muscle areas), and between fibre types (type IIA versus type I), accepting a significant difference at $P<0.05$. On the small number of occasions where the data were not normally distributed, Mann–Whitney *U*-tests were performed. The variance of quantitative features of specific fibre types was estimated within each muscle sample by calculating the coefficient of variability (CV) as: CV=(s.d./mean)×100 (Dubowitz and Sewry, 2007) (Table S1). To investigate whether muscle enzyme activities of fin whales scale allometrically with body mass, fibre-type histochemical and whole muscle biochemical muscle enzyme activities derived from present and past research (see Results) were correlated against body mass in a variety of terrestrial and marine mammals ranging in body size from the shrew (5 g) to the fin whale (12.5 tons on average in present study). Muscle enzyme data of each species were searched from the available locomotor (epaxial and hindlimb) muscles analysed in the specialized literature. To adjust for allometric differences due to body mass (BM), we scaled the enzyme activities to the estimated muscle tissue-specific resting metabolic rate (RMR) for each species. Based on the work of Wang et al. (2001), the scaling exponent for the RMR of individual tissues is more variable than for the whole body RMR. Therefore, instead of scaling enzyme activities with the whole body RMR, the estimated specific RMR for muscle tissue was used as $RMR=125\ BM^{-0.17}$ (Polasek et al., 2006) (Table S1).

RESULTS

Myosin-based muscle fibre types

Two resolvable bands were clearly separated in fin whale skeletal muscle by SDS-PAGE (Fig. 1A). Identification of these bands was examined by immunoblotting with anti-MHC MAbs (Fig. 1B). The fastest migrating band in the gels was labelled by MAbs BA-F8, BF-35 and S5-8H2, but not by MAbs SC-75 and SC-71. Based on the specificity of these MAbs (see Table 1), the two bands were identified as MHC IIA and MHC I, going from the slowest to the fastest migrating band (Fig. 1A).

Three fibre types were identified by inspection of muscle sections stained by immunohistochemistry (Table 1; Fig. 1C–F). Two were pure fibre types expressing a unique MHC (I and IIA), and the third was a hybrid fibre containing MHC I and MHC IIA (I+IIA fibres). Type I fibres reacted with MAbs BF-F8, BF-35 and S5-8H2, but not with MAbs SC-75 (not shown) and SC-71 (e.g. fibre '1' in Fig. 1C–F). Pure IIA fibres reacted strongly with MAbs SC-71, SC-75 (not shown) and BF-35, and were unstained with MAb S5-8H2, specific to all adult MHC isoforms except IIA (e.g. fibres '2' and '2′' in Fig. 1C–F). Hybrid I+IIA fibres were labelled with all five MAbs used here (e.g. fibres '3' and '3′' in Fig. 1C–F; result not shown for the MAb SC-75).

On the basis of visual examination of consecutive acid (pH 4.4) and alkaline (pH 10.3) myosin ATPase histochemical reactions, fin whale muscle fibre types could also be divided into three main staining intensities (Fig. 1G,H). In the acid pre-incubation, these stains were black (type I), white (type IIA) and intermediate (I+IIA), whereas in the alkaline pre-treatment, they were white (type I), dark (IIA) and medium (I+IIA). Thus, type I fibres were acid stable and alkaline labile (e.g. fibre labelled '1' in Fig. 1G,H). Type IIA were acid labile and alkaline stable (e.g. fibres '2' and '2′' in Fig. 1G,H). Again, hybrid I+IIA fibres had myosin ATPase activities intermediate to those of their respective pure MHC fibre types (e.g. fibres '3' and '3′' in Fig. 1G,H), but an objective delineation of these hybrid fibres was not always possible by visual inspection of myosin ATPase histochemistry. This limitation was confirmed because the percentage of hybrid I+IIA fibres delineated by myosin ATPase histochemistry in 20 muscle samples was significantly lower than the proportion of these fibres identified by immunohistochemistry with specific anti-MHC MAbs (mean±s.e.m., 3.0±0.5 vs 8.3±1.3%, $P<0.001$, paired *t*-test for dependent samples).

In general, the effect of the muscle location (e.g. middle versus caudal regions of the longissimus) on muscle variable analysed in the present study was not significant ($P>0.05$). Thus, further quantitative data are presented as pooled means of both muscle regions. Effects of sampling depth (e.g. superficial versus deep muscle areas) on muscle fibre type composition and muscle enzyme activities were significant ($P<0.05$, paired *t*-test for dependent samples). Myosin heavy chain composition, based on electrophoresis, differed significantly between

Journal of Experimental Biology (2018) 221, jeb177758. doi:10.1242/jeb.177758

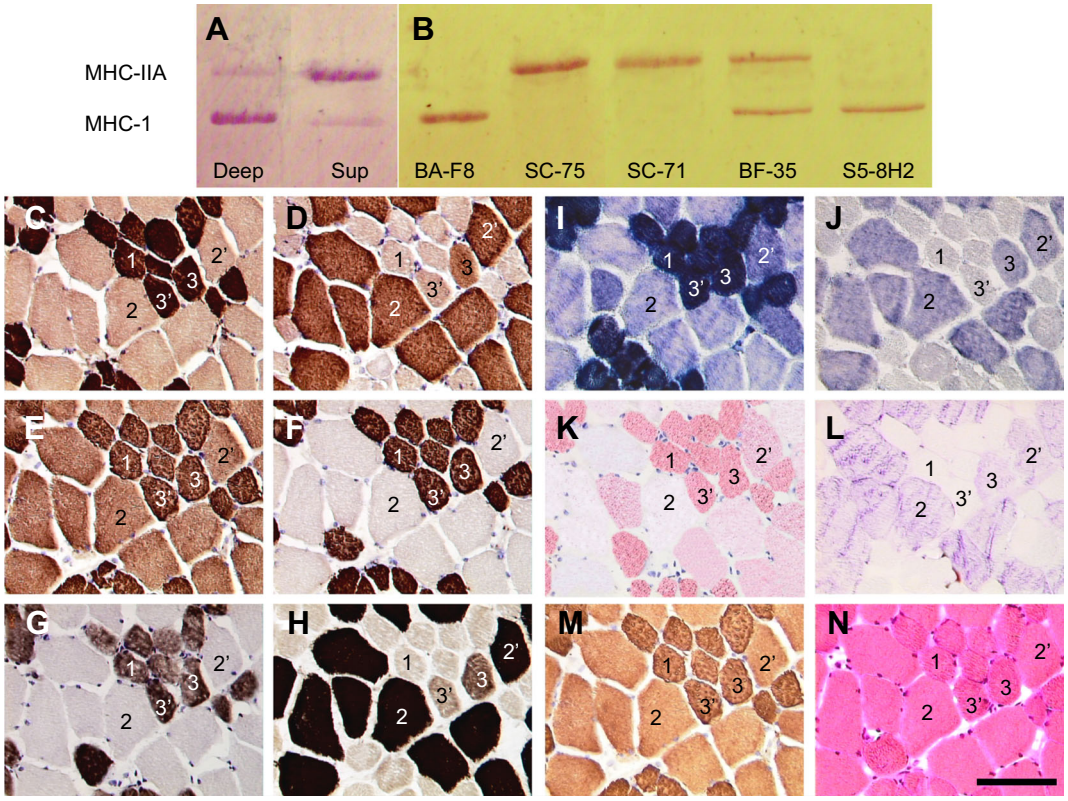

Fig. 1. Characterization of muscle fibre types of the fin whale (*Balaenoptera physalus*) according to the myosin heavy chain (MHC) isoform they express. (A) 8% SDS-PAGE of representative deep ('Deep') and superficial ('Sup') muscle samples showing two MHC bands with different migrating speeds. (B) Immunoblots stained with specific anti-MHC monoclonal antibodies [BA-F8 (anti MHC I), SC-75 (anti MHC IIA+IIX+IIB), SC-71 (anti MHC IIA), BF-35 (anti MHC I+IIA+IIB) and S5-8H2 (anti MHC I+IIX+IIB)], revealing that the two electrophoretically separated bands are identified as MHC-IIA and MHC-I isoforms going from the slowest (top) to the fastest (bottom) migrating bands. (C–N) Serial sections of a representative superficial sample of the longissimus dorsi muscle of *B. physalus* were stained for immunohistochemistry (C–F,M), enzyme histochemistry (G–J) and histology (K,L,N) of MHC-based fibre types: monoclonal antibodies BF-F8 (C), SC-71 (D), BF-35 (E) and S5-8H2 (F); acidic (G) and alkaline (H) pre-incubations of myosin ATPase; succinate dehydrogenase (I) and glycerol-3-phosphate dehydrogenase (J) histochemical enzyme activities; oil red O (K) and periodic acid–Schiff (L); immunohistochemistry with the anti-myoglobin monoclonal antibody MG-1 (M); and haematoxylin and eosin (N). Scale bar, 100 µm. The muscle fibres labelled '1' and '2' are pure fibres expressing MHCs I and IIA, respectively; the fibre labelled '2′' is a pure MHC-IIA fibre showing high SDH activity (I); the fibre labelled '3' is a hybrid fibre co-expressing MHC I +IIA with predominance of MHC-IIA on MHC-I; the fibre labelled '3′' is also a hybrid I+IIA fibre with dominance of MHC I versus MHC IIA, and showing weaker GPDH and PAS staining compared with previous hybrid fibre phenotype (3).

the two sampling depths of the muscle (Figs 1A and 2A). Deep regions of the muscle had significantly lower percentages of MHC IIA and higher proportions of MHC I than superficial areas of the muscle (P<0.001 in both). In consequence, the IIA-to-I MHC isoform ratio, used as a relative indicator of fast- versus slow-contracting profile of the muscle, was 3.3 times higher in superficial than in the deep region of the muscle (P<0.01). These electrophoretic data were corroborated by results of muscle fibre type composition based on immunohistochemistry (Fig. 2B). Deep regions of the muscle contained a significantly higher percentage of type I fibres, and a lower proportion of type IIA fibres than superficial areas (P<0.001 in both). The percentage of hybrid type I+IIA fibres was comparable at both sampling depths (P>0.05).

The patterns of fibre-type distribution also differed between the two sampling depths of the muscle. While samples removed from the superficial areas of the muscle showed a classical mosaic pattern, deep samples exhibited large and frequent fibre-type grouping of type I fibres (Fig. 3A,B).

Metabolic and morphological features of muscle fibre types

As the effect of sampling depth on metabolic and morphological properties of muscle fibre types was not significant (P>0.05), data in graphs are presented as pooled means of both regions (Fig. 4). On average, type I fibres exhibited higher SDH activities (104%) and lower GPDH activities (32%) than type IIA fibres (P<0.001 in both; Figs 1I,L and 4A). These enzyme activities were intermediate in type I+IIA hybrid fibres (result not shown). The GPDH/SDH ratio, used as an indicator of the relative glycolytic versus oxidative metabolic profile of muscle fibres, was three times higher in type IIA than in type I fibres (mean±s.e.m., 0.81±0.02 vs 0.27±0.01, P<0.001). Although staining intensity of the SDH enzyme was consistently high in all pure type I fibres, a spectrum from low to moderate staining intensities was perceived within pure type IIA fibres (e.g. fibres 2 and 2′ in Fig. 1I). This continuum of SDH histochemical activities within type IIA fibres was further confirmed by their higher variance range compared with type I fibres (average CV 1000, 112 vs 53, P<0.001, Mann–Whitney U matched pairs test). Furthermore, SDH activity and CSA of individual type IIA muscle fibres were inversely correlated on a per fibre basis (Fig. S1). Thus, the smaller the muscle fibre, the higher the SDH histochemical activity of this fibre-type population.

To investigate if the allometric trend of variations in muscle metabolic profiles that accompany larger body sizes (Kanatous et al., 2002; Polasek et al., 2006; Velten et al., 2013) is fibre-type

Journal of Experimental Biology (2018) 221, jeb177758. doi:10.1242/jeb.177758

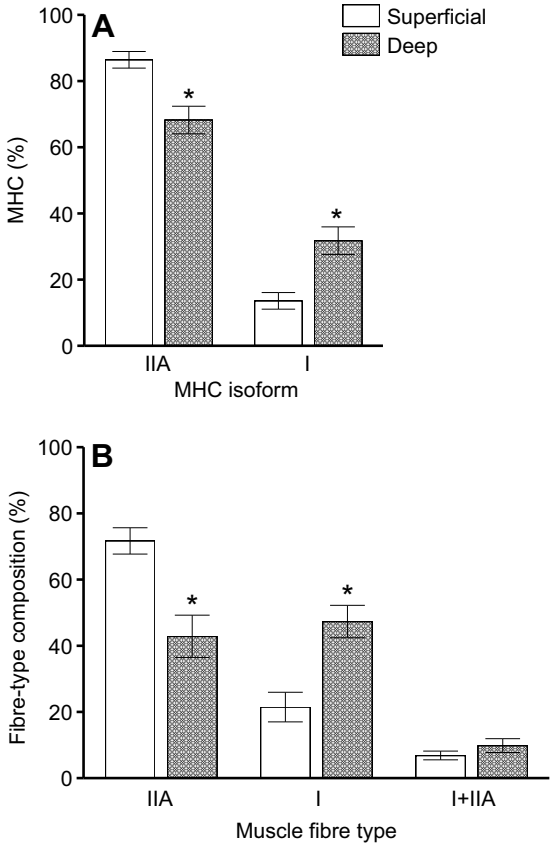

Fig. 2. Percentages of electrophoretically derived myosin heavy chain (MHC) isoforms and immunohistochemically identified muscle fibre types in superficial and deep regions of the longissimus muscle of four specimens of *B. physalus*. (A) MHC isoforms; (B) muscle fibre types. Data are pooled means±s.e.m. of N=10 samples/sampling depth; *significant difference (paired t-test for dependent samples).

specific, SDH and GPDH histochemical activities of IIA and I fibre-types obtained in the present study were compiled with a data set of locomotor muscles derived from previous research in a number of terrestrial mammals, ranging in body size from the rat (250 g) to the cow (500 kg) (Table S2). Both SDH and the GPDH/SDH enzyme ratio of type IIA fibres scaled with body mass (r=−0.73 and r=0.81, respectively, P<0.05 for both). The histochemical GPDH activity of both fibre types did not scale with body size, but the GPDH/SDH enzyme ratio of fast IIA fibres was significantly higher in fin whales compared with other terrestrial mammals (55%). Compared with the rat (Rivero et al., 1998), the species in the lowest range of body size, the difference of the GPDH/SDH enzyme ratio between fibre types (i.e. type IIA minus type I) was ∼12 times higher in fin whales.

Staining intensities of muscle sections stained for ORO (Fig. 1K), PAS (Fig. 1L) and MG-1 (Fig. 1M), used as indirect measurements of lipid, glycogen and Mb contents, respectively, were fibre-type specific in the fin whale locomotor muscle (Fig. 4B). Type IIA fibres stained less intensely for ORO and MG-1, and more intensely for PAS (e.g. fibres labelled '2' and '2′' in Fig. 1K–M) than type I fibres (e.g. fibre '1' in Fig. 1K–M), but an objective delineation of hybrid I+IIA fibres (e.g. fibres '3' and '3′' in Fig. 1K–M) was not possible by visual inspection. On average, type IIA fibres showed significantly lower ORO and MG-1 end-point optical density (OD_{ep}) (59 and 68%, respectively; P<0.001 for both) and higher PAS OD_{ep} (29%, P=0.01) than type I fibres. The ORO/PAS staining ratio, used as an indicator of the relative lipid-based versus glycogen-based metabolic profile of fibre types, was 3.5 times higher in type I than in type IIA fibres (4.77±0.85 vs 1.38±0.22, P<0.01).

The mean CSA of type I fibres was significantly smaller than that of type IIA fibres (∼60%, P<0.001; Fig. 4C). The variance range of the CSA of individual muscle fibres was significantly higher in type IIA than in type I fibres (CV 1000: 363±99 vs 235±59, P<0.001), as illustrated in Fig. S1. The average number of capillaries supplying the specific fibre types was significantly higher in type I fibres than in type IIA fibres, both in absolute (capillaries per fibre, ∼22%, P<0.05) and relative (capillaries per unit area, ∼210%, P<0.001) terms (Fig. 4D).

Whole muscle enzyme activities and myoglobin content

The metabolic profile of the fin whale locomotor muscle was also examined by biochemical analysis of LDH, CS and HAD enzyme activities, and [Mb] of muscle homogenates. We tested for the homogeneity of these metabolic indicators between muscle locations (e.g. middle versus caudal regions of the muscle). However, the effect of sampling depth on muscle enzyme activities and [Mb] was

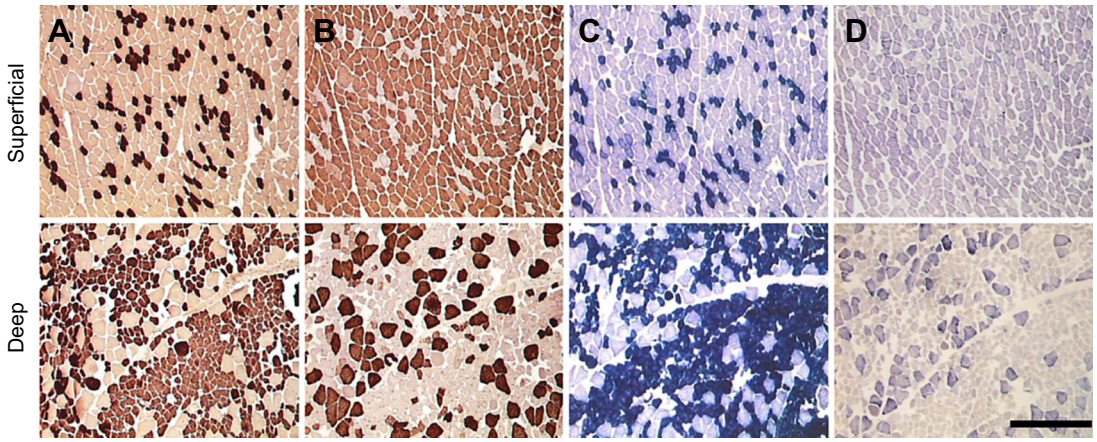

Fig. 3. Heterogeneity of contractile and metabolic phenotypes of the longissimus muscle of *B. physalus*. Low magnification serial sections of representative superficial (upper row) and deep (lower row) muscle regions were stained for immunohistochemistry with monoclonal antibodies BA-F8 (A), specific against MHC I, and SC-71 (B), anti MHC IIA, and for quantitative histochemistry of succinate dehydrogenase (C), an oxidative marker, and glycerol-3-phosphate dehydrogenase (D), used as a glycolytic indicator. Scale bar, 500 µm. Note the predominantly fast-glycolytic profile of the superficial region of the muscle compared with the slower and more oxidative design of the deep area of the same muscle.

Journal of Experimental Biology (2018) 221, jeb177758. doi:10.1242/jeb.177758

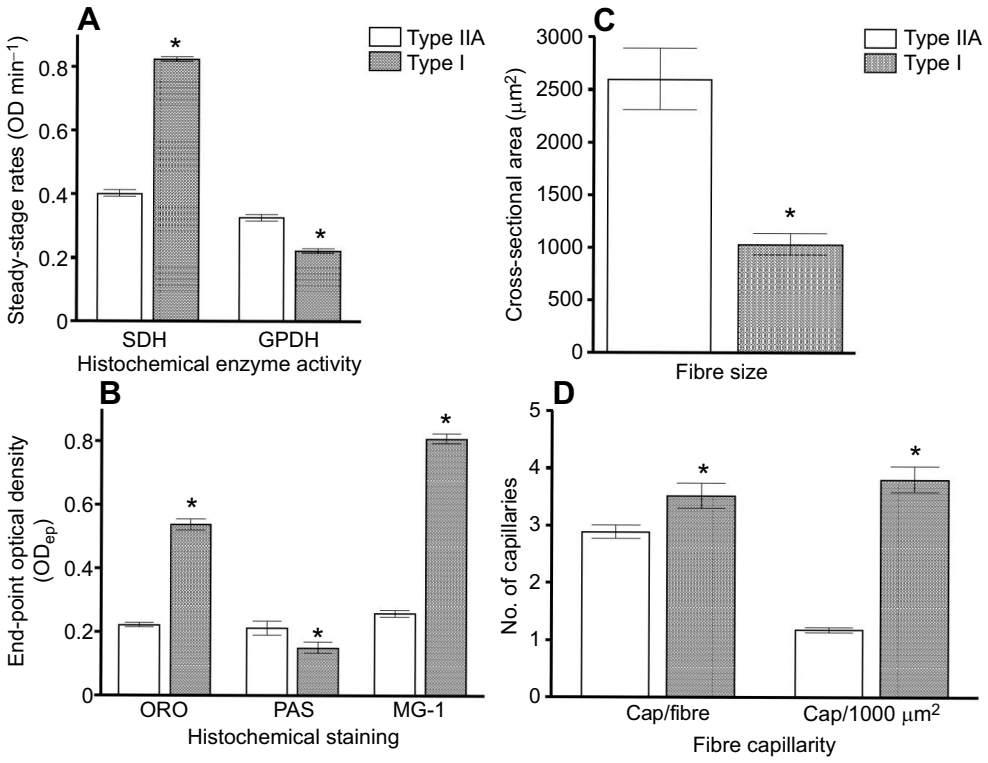

Fig. 4. Metabolic and morphological features of muscle fibre types of the longissimus muscle of four specimens of *B. physalus*. (A) Steady-state rates (OD min^{-1}) for quantitative histochemistry of muscle enzymes succinate dehydrogenase (SDH) and glycerol-3-phosphate dehydrogenase (GPDH); (B) end-point optical densities (OD_{ep}) for densitometry of histochemical stains oil red O (ORO), periodic acid–Schiff (PAS), and immunostaining of the anti-myoglobin monoclonal antibody MG-1, (C) cross-sectional area (μm^2) and (D) capillaries (Cap) (in both absolute number per fibre and relative number per area unit) of the two main fibre types (IIA and I) of the longissimus muscle of four fin whales (*B. physalus*). Data are pooled means±s.e.m. of *N*=20 samples; *significant difference (paired *t*-test for dependent samples). Hybrid I+IIA fibres are excluded due to their low frequency (8% on average) and inconsistency (absent in 25% of samples).

significant (Table 2). The mean LDH activity and mean LDH/CS enzyme ratio were higher (38 and 65%, respectively), and the mean CS and HAD activities were lower (19 and 15%, respectively) in superficial areas than in deep regions of the muscle. No significant depth-related variation in the CS/HAD enzyme activity ratio was observed. The mean [Mb] was significantly higher in deep areas than in superficial regions of the muscle (30% on average). As a consequence, superficial areas of the muscle showed a predominantly glycolytic versus oxidative metabolic profile, whereas the deep regions of the muscle were (comparatively) highly oxidative and weakly glycolytic (Fig. 3C,D).

Muscle enzyme activities of locomotor (epaxial and hindlimb) muscles were compared in terrestrial and marine mammals that cover seven orders of magnitude in body masses (Table 3). The activity of the anaerobic glycolytic enzyme LDH increased as body mass increased, whereas the activities of oxidative enzymes CS and HAD decreased significantly as body size increased. To adjust for these allometric differences due to body mass, muscle enzyme activities from these species were scaled to the muscle tissue-specific RMR (Fig. 5). When scaled to muscle-specific RMR, the activities of the three muscle enzymes analysed increased significantly as a function of body mass. Like in other sprinters such as the African cheetah and the black wildebeest, the LDH/RMR enzyme activity in superficial samples of the fin whale locomotor muscle was ∼43% higher than that predicted for a mammal of comparable size (Fig. 5A). The HAD/RMR enzyme activity in deep samples of the fin whale swimming muscle also resulted in ∼34% greater than predicted value calculated for a mammal of comparable body mass, but was comparable to values reported in Weddell seal, and terrestrial herbivores such as the black wildebeest and horses (Fig. 5C).

Table 2. The effects of sampling depth on muscle metabolic indicators of fin whale (*Balaenoptera physalus*)

	Muscle sampling area		
Variable	Superficial	Deep	*P*-values
LDH (µmol g^{-1} min^{-1})	1489±88	1113±77	*P*=0.004
CS (µmol g^{-1} min^{-1})	15.5±1.8	19.1±1.5	*P*<0.001
HAD (µmol g^{-1} min^{-1})	23.4±1.5	27.4±3.1	*P*=0.007
LDH/CS	97.4±7.2	58.9±4.9	*P*<0.001
CS/HAD	0.66±0.06	0.70±0.07	*P*=0.2
[Mb] (mg g^{-1})	27.2±1.8	30.3±1.6	*P*=0.002

Muscle enzyme activities [lactate dehydrogenase (LDH), citrate synthase (CS) and β-hydroxyacyl coenzyme A dehydrogenase (HAD)], muscle enzyme ratios [ratio of LDH to CS (LDH/CS) and ratio of CS to HAD (CS/HAD)], and myoglobin concentration [Mb] of the longissimus muscle of four specimens of *B. physalus*. Data are pooled means±s.e.m. of *N*=10 samples/sampling depth; *P*-values denote significance of differences between sampling depths (paired *t*-test for dependent samples).

DISCUSSION

Significance of the fin whale locomotor muscle profile

The fin whale locomotor muscle, composed of approximately 80% of fast-twitch fibres (see Fig. 2), and a predominantly glycolytic profile (see Table 2), is comparable to that of terrestrial mammalian sprinters (Williams et al., 1997; Kohn et al., 2011a) and high-performance, steady swimming fish (Ellerby et al., 2000). To our knowledge, both the increased proportion of fast MHC-IIA (∼90% in superficial regions in adult whales), and the enhanced LDH/CS muscle enzyme ratio (∼100 in the same muscle area) of the fin whale longissimus muscle are the highest values reported in epaxial muscle of any marine mammal (Kanatous et al., 2002; Polasek et al., 2006). Considered as relatively shallow-diving animals despite being able to dive deeper and for longer periods (Croll et al., 2001), fin whales have a faster and more glycolytic locomotor muscle profile than other short-duration, shallow diving mammals (Bello et al., 1985; Watson et al., 2003; Polasek et al., 2006). The predominantly fast-glycolytic profile of their propulsive muscles

Journal of Experimental Biology (2018) 221, jeb177758. doi:10.1242/jeb.177758

Table 3. Scaling of enzyme activities in mammalian skeletal muscles

Species	Mass (kg)	LDH	CS	HAD	Data source
Shrew	0.005	158	65.0	80.5	Emmett and Hochachka, 1981
Deer mouse	0.014	686	45.0	69.5	Emmett and Hochachka, 1981
Mouse	0.021	550	86.0	76.2	Lui et al., 2015; Southern et al., 2017
Wistar rat	0.335	500	20.0	8.0	Li et al., 2016; Yoshida et al., 2007
Guinea-pig	0.61	904	25.5	19.9	Emmett and Hochachka, 1981
Rabbit	2.9	842	2.9	2.7	Zomeño et al., 2010
Dog	9.2	480	43.3	6.0	Polasek et al., 2006
Caracal	11.0	346	6.2	1.7	Kohn et al., 2011a
Rhesus monkey	11.5	1325	15.5	5.2	Emmett and Hochachka, 1981
Habour seal	46.1	1002	32.9	26.9	Polasek et al., 2006
African cheetah	50.0	1929			Williams et al., 1997
Human (runner)	63.7	290	25.0	28.0	Kohn et al., 2007
Human (sprinter)	73.4	361	35.0	29.9	MacDougall et al., 1998
Pig	120	2204	6.4	3.5	Lefaucheur et al., 2004
Deer	135	1530	38.5	12.5	Emmett and Hochachka, 1981
Lion	140	227	6.7	2.1	Kohn et al., 2011a
Black wildebeest	155	2518	31.5	56.0	Kohn et al., 2011b
Cow	370	2146	7.2	6.6	Emmett and Hochachka, 1981
Weddell seal	404	563	12.0	48.5	Kanatous et al., 2002
Racehorse	460	1200	39.0	29.0	Lovell and Rose, 1991
Endurance horse	500	863	27.4	40.7	Rivero et al., 1995
Meat cow	1000	2055	12.7	1.8	Emmett and Hochachka, 1981
Fin whale (superficial)	10,540	1490	15.5	23.4	Present study
Fin whale (deep)	10,540	1113	19.1	27.4	Present study
		r=0.46	r=−0.58	r=−0.46	
		P=0.02	P=0.003	P=0.02	

Mean muscle enzyme activities (μmol g^{-1} min^{-1}) (see footnote to Table 2 for key) in locomotor (epaxial or hindlimb) muscles from a variety of mammalian species ranging in size from the shrew (5 g) to the fin whale (10.5 tons). These compiled data were selected from a bibliographical search of studies with similar methodologies. Linear relationships, and their significance levels (P-values) of enzyme activities against body mass (log body mass, in kg) were estimated by correlation coefficients (r).

explains why the fin whale is the fastest swimmer among rorqual whales (Bose and Lien, 1989).

As in the present study, the GPDH staining of type II fibres was darker than that of type I fibres in cetaceans (Suzuki et al., 1983; Velten et al., 2013). Quantitatively, this difference was of comparable magnitude to that reported in terrestrial mammals (Table S2). In the present study, the average SDH activity of muscle fibres was ∼52% lower in type IIA than in type I fibres. A difference of similar magnitude has been reported in locomotor muscles of cetaceans (Suzuki et al., 1983; Kielhorn et al., 2013; Velten et al., 2013). However, the difference of the oxidative capacity between type IIA and type I fibres is usually modest in terrestrial mammals (∼10% lower in IIA versus I fibres on average; Table S2). The difference of GPDH/SDH enzyme ratio, which is an indirect measure of the relative contribution of anaerobic versus aerobic metabolism in muscle cells, between the two major fibre types of the fin whale showed the highest value reported in locomotor muscles of any mammal (Table S2). This observation indicates that, compared with terrestrial mammals, the abundant type IIA fibres of the fin whale locomotor muscle have an extremely high-glycolytic potential relative to a very diminished aerobic capacity. In the present study, the SDH histochemical activity of type I muscle fibres did not scale with body mass and, in the fin whale, showed the highest value of any terrestrial mammal (Table S2). This observation could indicate that type I fibres of the fin whale have mitochondrial densities much higher than would be predicted from an allometric consideration of its extreme body size (Hoppeler and Weibel, 2005).

In the present study, a fraction of the immunohistochemically characterized hybrid I+IIA fibres in the fin whale stained with GPDH staining (e.g. fibre labelled ‘3’ in Fig. 1J). Present results also confirm that mATPase histochemistry, compared with immunohistochemistry, underestimates hybrid fibres co-expressing different MHC isoforms (Rivero et al., 1996a; Acevedo and Rivero, 2006). Thus, the abundant slow-glycolytic muscle fibres described in pilot whales (Velten et al., 2013) might well be a consequence of this limitation of the fibre-typing method used (for relevant discussion, see Watson et al., 2003).

Few studies have simultaneously examined endogenous substrates in muscle fibre types of marine mammals (Suzuki et al., 1983). The present results show that, compared with type I fibres, type IIA fibres of the fin whale have higher glycogen (revealed by PAS stain), and lower lipid (ORO stain) and Mb (MG-1 immunostaining) contents. The co-localization of PAS with GPDH stains observed in fin whale muscle fibre types suggests a greater dependence on glycogen as an endogenous source of energy in their abundant type IIA fibres compared with type I fibres. The relatively low PAS staining intensity of muscle fibres of the fin whale, compared with athletic terrestrial species such as dogs (Acevedo and Rivero, 2006) and horses (Quiroz-Rothe and Rivero, 2001), could be related to the low carbohydrate content of the diet of these cetaceans (Kawamura, 1980), and/or exhaustion during their stranding. In agreement with the present study, the lipid content of muscle fibres of beaked whales was ∼4.5 times higher in type I than in type IIA fibres (Velten et al., 2013). Very fine granules of lipids were also found in type I myofibres, but not in type II myofibres in the longissimus muscle of dolphins (Suzuki et al., 1983). The co-localization of ORO with SDH staining intensities observed in muscle fibre types of fin whales, indicates that lipids are the main aerobic fuel in their type I fibres. This is reinforced by the parallel relationship between MG-1 and SDH staining intensities observed in the two muscle fibre types, suggesting co-localization

Journal of Experimental Biology (2018) 221, jeb177758. doi:10.1242/jeb.177758

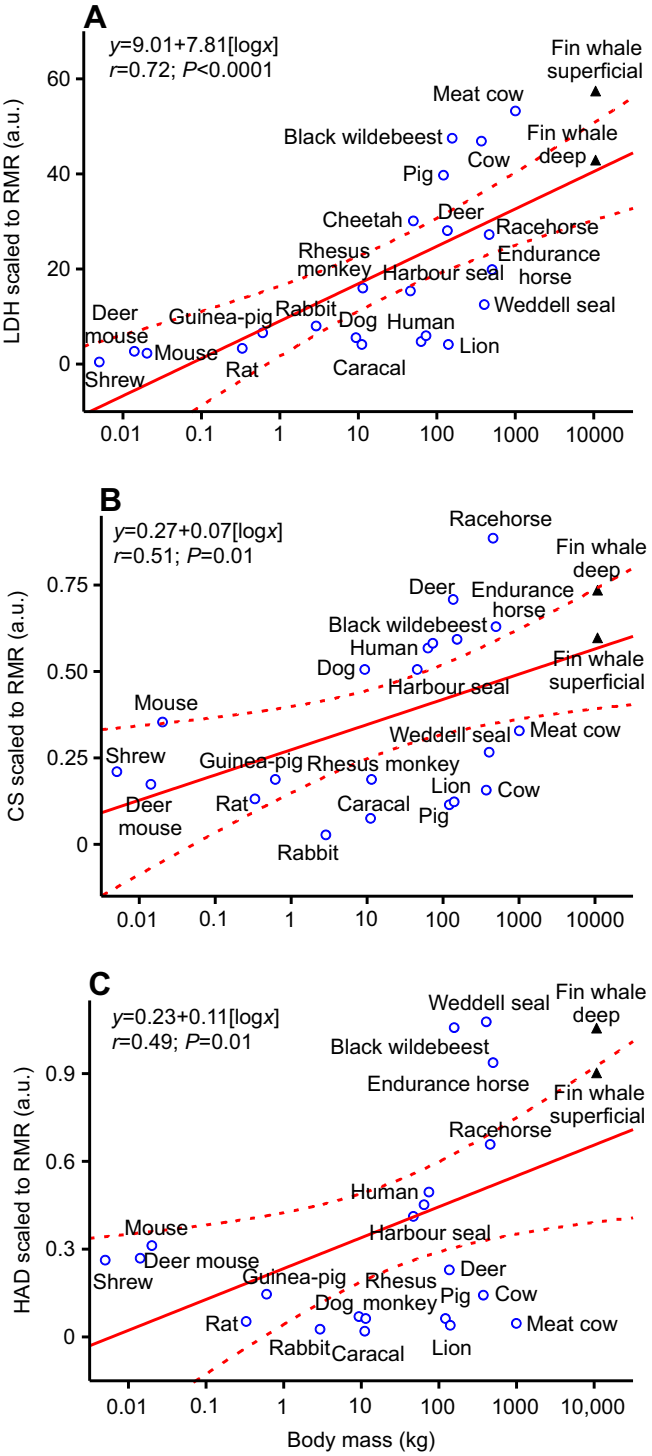

Fig. 5. Plots of muscle enzyme activities scaled to muscle-specific resting metabolic rate against body mass. (A) LDH; (B) CS; (C) HAD; see footnote to Table 2 for key. Resting metabolic rate (RMR)=125 $BM^{-0.17}$, where BM is the body mass in kg; RMR is given in kJ kg^{-1} day^{-1}. The linear relationships (regression lines and 95% confidence intervals) were generated from the enzyme activities of locomotor (epaxial and hindlimb) muscles from a variety of terrestrial and marine mammals ranging in body mass from the shrew (5 g) to the fin whale (10.5 tons; filled triangles). See Table 3 for data sources. a.u., arbitrary units.

of Mb with mitochondria as already verified in rat skeletal muscle (Yamada et al., 2013). In comparison with terrestrial mammals, which have a larger proportion of mitochondria that are subsarcolemmal (Hoppeler et al., 1987), in marine mammals most of the mitochondria (~80%) have an interfibrillar distribution (Kanatous et al., 2002; Watson et al., 2007; Velten et al., 2013). Qualitative observations of the present study confirmed this result in fin whales, as shown by the homogeneous staining of the SDH histochemical activity across the transverse section of the fibres, particularly in type I fibres (see Fig. 1I). This feature could affect oxygen diffusion capacity in marine mammals by (1) increasing the diffusion surface area of mitochondria, and (2) reducing the intracellular distance between mitochondria and Mb.

Morphological features observed in the present study reinforce the idea that the fin whale locomotor muscle has the typical profile of a high-performance sprinter. Its relatively small fibre size (Table S3) is comparable to that seen in innate sprinters such as greyhound dogs (Agüera et al., 1990) and thoroughbred racehorses (Rivero et al., 2007). It is also comparable to that seen in short-duration, shallow dives (Bello et al., 1985; Kanatous et al., 2001), but clearly smaller than that reported in deep-diving marine mammals (Kanatous et al., 2002; Williams and Noren, 2011; Kielhorn et al., 2013; Velten et al., 2013). It has been postulated that small muscle fibre size raises muscle basal metabolic rate by increasing the relative surface area across which ions must be pumped to maintaining the cell's membrane potential (Jimenez et al., 2011). Under these conditions, small fibre size, and the potential concomitant higher metabolic costs associated with maintaining ionic homeostasis, would appear to be beneficial to increasing the overall metabolic rate. This feature may be especially important to a sprinter (relatively short- and shallow diver such as the fin whale) that utilizes very high energetic demands during foraging dives (Potvin et al., 2012).

Like other marine mammals (Reed et al., 1994; Kanatous et al., 2002, 2001), fin whale locomotor muscle has a lower absolute number of capillaries supplying muscle fibres compared with terrestrial mammals (Table S3). In relative terms, however, expressed per unit of CSA, the average number of capillaries in contact with a fibre in the fin whale is comparable to those of terrestrial mammals (Table S3) and clearly intermediate in between those of shallow- versus deep-divers (Kanatous et al., 2002, 2001). The present results also showed that the average number of capillaries around a fibre in the fin whale is significantly higher in type I than in type IIA fibres, but while this difference was of comparable magnitude in fin whales (e.g. IIA-to-I ratio, 0.82) and other terrestrial mammals (e.g. 0.92) when the number of capillaries was expressed in absolute terms, it was approximately three times lower in fin whales (0.31) than in terrestrial animals (0.92) when the capillary supply of a fibre was expressed in relation to its mean CSA (Table S3). A similar difference was present between fin whales and a variety of pinniped species (Reed et al., 1994). These differences mean that, compared with terrestrial mammals and pinnipeds, the relative number of capillaries around a fibre in the fin whale locomotor muscle is much lower for type IIA fibres and much higher for type I fibres. Also compared with terrestrial mammals, as type I fibres of the fin whale have an enhanced aerobic capacity and a reduced fibre size (see previous discussion), this observation implies that this fibre-type maximizes its increased aerobic capacity and mitochondrial density with greater capillary supply per unit of area. In contrast, type IIA fibres link their decreased aerobic capacity, enhanced anaerobic capacity and high glycogen content with decreased capillary supply relative to fibre CSA. As this fibre-type also has limited lipid content, its relatively low capillarity suggests that, as in terrestrial mammals, the fuel for these cells must be supplied by glycogen catabolism as exercise intensity is maximal or supramaximal (Hoppeler and Weibel, 1998).

The present study confirmed the relatively low [Mb] reported in skeletal muscle of baleen whales (Noren and Williams, 2000). Although this feature contradicts allometric trends of enhanced Mb content that accompany larger body sizes, as demonstrated in toothed whales (Noren and Williams, 2000), it is consistent with both the limited dive durations (Croll et al., 2001) and the purported high energetic cost of foraging in mysticetes (Potvin et al., 2012).

A recent study reported that the extreme deep-diver beaked whales have a sprinter fibre-type profile composed of ~80% type II fibres with extremely low mitochondrial content (Velten et al., 2013). However, this enhanced fast-glycolytic profile occurred with larger fibre size and higher [Mb] compared with the present results. It was hypothesized that this unusual muscle profile could increase the animal's total body oxygen stores (Velten et al., 2013).

Division of labour in the fin whale swimming muscle

Compared with superficial regions, deep regions of the fin whale muscle longissimus dorsi have a muscle phenotype significantly slower, more oxidative, and (relatively) less glycolytic. Watson et al. (2003) showed that the distribution of type I fibres tended to increase with respect to the depth in epaxial muscles of harbour seals. A similar regional variation in fibre-type composition across the transverse section of the entire epaxial musculature was also reported in adult bottlenose dolphins (Dearolf et al., 2000). Bello et al. (1985) reported important differences in the architectural design of the dorsal and ventral axial muscle in dolphins, where the epaxial muscles appear to be designed to optimize velocity and displacement (i.e. longer fibres). Watson et al. (2007) reported in epaxial muscles of the harbour seal that V_{mt} was significantly greater in samples collected from deep (6.03%) compared with superficial regions (4.95%). Polasek and Davis (2001) also found in dolphins and a false killer whale that the interior (deep areas) of the epaxial muscle lying closest to the vertebrae, contain a significantly higher (11%) mean [Mb] than the exterior (superficial areas) of the same muscle.

It seems evident that depth-related variations of muscle characteristics observed in the current study have clear functional significance, indicating a division of labour between muscle sub-volumes, as reported in terrestrial mammals (Lopez-Rivero et al., 1992). As these differences include contractile and metabolic properties of muscle, they may reflect force generation and energy metabolism within the muscle during dorsal–ventral flexion of the spine associated with thrust generation during swimming. Thus, the presumably eccentric muscle contraction and the comparatively slower and more oxidative profile of deep compartments of the fin whale longissimus muscle seems to be involved in the active–passive extension of the spine during sustained, low-intensity swimming necessary to travelling (migration) and non-foraging dives. However, the almost exclusive concentric (active) muscle contraction, revealed by its extremely high fast-glycolytic profile, of the superficial compartment of this muscle suggests its involvement in the rapid (explosive) and highly energetically costly spinal extension (produced by the upstroke) during the lunge and high-speed pursuit.

Regional variations seen within the fin whale longissimus muscle may also reflect mechanical differences in the way forces generated by this muscle are transmitted to the skeleton to actuate the propulsive movements of the tail. The muscle architecture of the epaxial (upstroke) muscles has been described in cetaceans (Bello et al., 1985; Pabst, 2000). Longissimus muscle fibres insert (partially) via the superficial tendon onto the neural spines of thoracic and lumbar vertebrae, but the vast majority of these tendon's fibres become woven into, and form part of, the helically wound subdermal connective tissue sheath (Pabst, 2000). This design represents a unique morphological construct of cetaceans that increase tendon excursion of the muscle and, hence, the moment arm of its force (Pabst, 2000). In view of the alignment of muscle architecture and fibre types in mammals (Graziotti et al., 2012), the abundance of fast-glycolytic fibres in the superficial region of the muscle implies the presence of long fibres with small pinnation angles, whereas the slower and more oxidative phenotype of the deep compartment implies shorter fibres with greater pinnation angles. Based on these differences, it seems reasonable to hypothesize that the superficial region of the muscle (long fibres, low pinnation) would have a greater displacement advantage, or tendon excursion, than the shorter fibres with higher pinnation of the deep region of the muscle. Thus, the superficial region of the muscle would optimize velocity and displacement through a higher amplitude of the fluke's upstroke during high-speed and burst swimming. In contrast, the shorter force's moment arm of the deep region of the longissimus suggests less potential for excursion changes, which is a more favourable design for low-speed and steady swimming.

In rorqual whales, feeding and locomotion are integrated in lunge-feeding (Potvin et al., 2012). Its ventral groove blubber (VGB) musculature is arranged into two strata with different architectural and histological features (Orton and Brodie, 1987; Shadwick et al., 2013). In fin whales, the deep (longitudinal) layer is almost exclusively composed of slow oxidative fibres with low extensibility, suggesting a postural role for load control during engulfment. In contrast, the superficial (oblique) compartment contains mixed populations of slow and fast fibres with high extensibility and abundant elastin, allowing the muscle to accommodate large deformation of the VGB during engulfment and to work actively in water filtration and purging after engulfment. Recent simulated biomechanical studies concluded that lunge-feeding is disproportionally costly for baleen whales with extreme body sizes (Potvin et al., 2009, 2012). Physiological demands of lunge-feeding are maximal during mouth opening in VGB musculature (Potvin et al., 2012), and rival those of athletic terrestrial mammals during maximal effort (Weibel and Hoppeler, 2005). The maximum metabolic rate (MMR), which is a direct measure of the maximum aerobic capacity of air-breathing terrestrial mammals (Weibel and Hoppeler, 2005), is exceeded in the fin whale during mouth opening, revealing the magnitude of the oxygen deficit that accumulates during the most demanding phase of engulfment (Potvin et al., 2012). At the upper extreme of body weight in the (extant) range of 25 to 27 m of blue whales, the rate of energy expenditure is most demanding, i.e. reaching MMR levels over several seconds (Potvin et al., 2012).

Allometric considerations of the fin whale locomotor muscle

Our results clearly indicated that adult fin whale locomotor muscles only express the two slowest MHC isoforms (I and IIA) of the complete inventory and expression pattern well-known in adult mammalian skeletal muscles (Schiaffino and Reggiani, 2011). This observation confirms previous studies in pinnipeds (Kanatous et al., 2002; Watson et al., 2003), but to our knowledge it represents the first description in a large cetacean. The lack of expression of the fastest MHC isoforms (IIX and IIB) in locomotor muscles of fin whales (present results) and other marine mammals (Kanatous et al., 2002; Watson et al., 2003) is not surprising, because the essential conditions for feeding and hunting among marine species also require that locomotion speed becomes virtually independent

of body size (Schiaffino and Reggiani, 2011). As pointed out by A.V. Hill (Hill, 1950), this implies that locomotor muscles of small-size animals must be able to shorten faster than those from large-size animals.

By means of a meta-analysis, the scaling of glycolytic and oxidative muscle enzymes has been closely assessed in the present study in between-species comparisons of terrestrial and marine mammals varying greatly in body size. The activity of the glycolytic enzyme LDH increased as body size increased (see Table 3), confirming that the larger the animal, the higher the glycolytic potential of its locomotor muscles (Emmett and Hochachka, 1981) (Fig. 5A). In contrast, the activities of the enzymes functioning in oxidative metabolism (CS and HAD) decreased as body weight increased (Table 3). Nevertheless, these linear relationships yield negative slopes (around −0.10) that were less than the allometric exponent (−0.17) typically used for muscle RMR (Polasek et al., 2006). These data imply that the scope for muscle aerobic activity in large mammals is greater than in small mammals, a result previously obtained by Emmett and Hochachka (1981), and confirmed in the present study (see Fig. 5B,C). Interestingly, when scaled to muscle-specific RMR, the activity of the glycolytic enzyme LDH in the superficial region of the fin whale locomotor muscle and the activity of the oxidative enzyme HAD in the deep region of this muscle, were higher than predicted from an allometric perspective (Fig. 5A, C). Again, this enhanced anaerobic capacity seems to be a desirable muscle characteristic for the extremely high power requirements of burst work during lunge (Potvin et al., 2012) and high-speed swimming (Ford and Reeves, 2008), whereas the high HAD/RMR enzyme activity suggests an enhanced lipid-based metabolism, which seems to be suitable to the power requirements of sustained performance during long-distance migrations. These features show that the locomotor muscle of the fin whale can generate great force and speed, and also has the potential to withstand fatigue for longer periods of time, explaining clearly why fin whales can reach and sustain greater swimming speeds than other rorqual whales.

Conclusions

Simulated biomechanical studies have provided unprecedented insights that the ram-feeding strategy (lunge-feeding) is disproportionally costly for baleen whales with extreme body size (Potvin et al., 2009, 2012), but until now data were lacking on the functional morphology and metabolism of their locomotor muscles. This paper has shown that the fin whale locomotor muscle displayed a predominantly fast-glycolytic phenotype dominated by abundant type IIA fibres with extremely high glycolytic potential, low oxidative capacity, reduced fibre size, and low number of capillaries. This sprinter's profile appears to satisfactorily match physiological demands of lunge-feeding, when the rate of energy expenditure reaches MMR levels over several seconds (Potvin et al., 2012). The study has also proved that superficial and deep compartments of the fin whale epaxial musculature are not homogeneous in structural and metabolic profiles, suggesting a division of labour for rapid, highly energetically costly actions during the lunge and fast swimming (superficial region), and low-intensity, sustained swimming during non-foraging dives (deep region). Finally, the study has also confirmed that the fin whale swimming muscle only expresses the two slowest MHC isoforms I and IIA, displaying anaerobic (glycolytic) and aerobic (lipid-based) metabolic capabilities higher than would be expected from an allometric consideration of its extreme body size. The relationships between muscle metabolism and body mass were fibre-type specific.

Competing interests
The author declares no competing or financial interests.

Funding
Funding was provided by the Andalusian Research Programme (Group CTS/179).

Supplementary information
Supplementary information available online at
http://jeb.biologists.org/lookup/doi/10.1242/jeb.177758.supplemental

References

Acevedo, L. M. and Rivero, J.-L. L. (2006). New insights into skeletal muscle fibre types in the dog with particular focus towards hybrid myosin phenotypes. *Cell Tissue Res.* **323**, 283-303.
Agüera, E., Diz, A., Vazquez-Auton, J. M., Vivo, J. and Monterde, J. G. (1990). Muscle fibre morphometry in three dog muscles of different functional purpose in different breeds. *Anat. Histol. Embryol.* **19**, 289-293.
Bello, M. A., Roy, R. R., Martin, T. P., Goforth, H. W. and Edgerton, V. R. (1985). Axial musculature in the dolphin (*Tursiops truncatus*): some architectural and histochemical characteristics. *Mar. Mam. Sci.* **1**, 324-336.
Blanco, C. E., Sieck, G. C. and Edgerton, V. R. (1988). Quantitative histochemical determination of succinic dehydrogenase activity in skeletal muscle fibres. *Histochem. J.* **20**, 230-243.
Bose, N. and Lien, J. (1989). Propulsion of a fin whale (*Balaenoptera physalus*): why the fin whale is a fast swimmer. *Proc. R. Soc. Lond. B Biol. Sci.* **237**, 175-200.
Boyd, I. L., Bevan, R. M., Woakes, A. J. and Butler, P. J. (1999). Heart rate and behavior of fur seals: implications for measurement of field energetics. *Am. J. Physiol.* **276**, H844-H857.
Brodie, P. F. (1993). Noise generated by the jaw actions of feeding fin whales. *Can. J. Zool.* **71**, 2546-2550.
Brooke, M. H. and Kaiser, K. K. (1970). Muscle fiber types: how many and what kind? *Arch. Neurol.* **23**, 369-379.
Croll, D. A., Acevedo-Gutiérrez, A., Tershy, B. R. and Urbán-Ramirez, J. (2001). The diving behavior of blue and fin whales: is dive duration shorter than expected based on oxygen stores? *Comp. Biochem. Physiol. A Mol. Integr. Physiol.* **129**, 797-809.
Dearolf, J. L. (2003). Diaphragm muscle development in bottlenose dolphins (*Tursiops truncatus*). *J. Morphol.* **256**, 79-88.
Dearolf, J. L., McLellan, W. A., Dillaman, R. M., Frierson, D., Jr. and Pabst, D. A. (2000). Precocial development of axial locomotor muscle in bottlenose dolphins (*Tursiops truncatus*). *J. Morphol.* **244**, 203-215.
Dubowitz, V. and Sewry, C. A. (2007). *Muscle Biopsy: A Practical Approach*. Edinburgh, UK: Saunders Elsevier.
Ellerby, D. J., Altringham, J. D., Williams, T. and Block, B. A. (2000). Slow muscle function of Pacific bonito (*Sarda chiliensis*) during steady swimming. *J. Exp. Biol.* **203**, 2001-2013.
Emmett, B. and Hochachka, P. W. (1981). Scaling of oxidative and glycolytic enzymes in mammals. *Respir. Physiol.* **45**, 261-272.
Ford, J. K. B. and Reeves, R. R. (2008). Fight or flight: antipredator strategies of baleen whales. *Mammal. Rev.* **38**, 50-86.
Geraci, J. R. and Lounsbury, V. J. (2005). *Marine Mammals Ashore: A Field Guide for Strandings*. Baltimore, MD: National Aquarium in Baltimore.
Goldbogen, J. A., Calambokidis, J., Croll, D. A., Harvey, J. T., Newton, K. M., Oleson, E. M., Schorr, G. and Shadwick, R. E. (2008). Foraging behavior of humpback whales: kinematic and respiratory patterns suggest a high cost for a lunge. *J. Exp. Biol.* **211**, 3712-3719.
Goldbogen, J. A., Calambokidis, J., Shadwick, R. E., Oleson, E. M., McDonald, M. A. and Hildebrand, J. A. (2006). Kinematics of foraging dives and lunge-feeding in fin whales. *J. Exp. Biol.* **209**, 1231-1244.
Graziotti, G. H., Chamizo, V. E., Ríos, C., Acevedo, L. M., Rodríguez-Menéndez, J. M., Victorica, C. and Rivero, J.-L. L. (2012). Adaptive functional specialisation of architectural design and fibre type characteristics in agonist shoulder flexor muscles of the llama, *Lama glama*. *J. Anat.* **221**, 151-163.
Guth, L. and Samaha, F. J. (1969). Qualitative differences between actomyosin ATPase of slow and fast mammalian muscle. *Exp. Neurol.* **25**, 138-152.
Halsey, L. G., Butler, P. J. and Blackburn, T. M. (2006). A phylogenetic analysis of the allometry of diving. *Am. Nat.* **167**, 276-287.
Hill, A. V. (1950). The dimensions of animals and their muscular dynamics. *Science* **38**, 209-230.
Hoppeler, H. and Weibel, E. R. (1998). Limits for oxygen and substrate transport in mammals. *J. Exp. Biol.* **201**, 1051-1064.
Hoppeler, H. and Weibel, E. R. (2005). Scaling functions to body size: theories and facts. *J. Exp. Biol.* **208**, 1573-1574.
Hoppeler, H., Kayar, S. R., Claassen, H., Uhlman, E. and Karas, R. H. (1987). Adaptive variation in the mammalian respiratory system in relation to energetic demand. III. Skeletal muscles: setting the demand for oxygen. *Respir. Physiol.* **69**, 27-46.

Jimenez, A. G., Dasika, S. K., Locke, B. R. and Kinsey, S. T. (2011). An evaluation of muscle maintenance costs during fiber hypertrophy in the lobster *Homarus americanus*: are larger muscle fibers cheaper to maintain? *J. Exp. Biol.* **214**, 3688-3697.

Kanatous, S. B., Elsner, R. and Mathieu-Costello, O. (2001). Muscle capillary supply in harbor seals. *J. Appl. Physiol.* **90**, 1919-1926.

Kanatous, S. B., Davis, R. W., Watson, R., Polasek, L., Williams, T. M. and Mathieu-Costello, O. (2002). Aerobic capacities in the skeletal muscles of Weddell seals: key to longer dive durations? *J. Exp. Biol.* **205**, 3601-3608.

Kawamura, A. (1980). A review of food balaenopterid whales. *Sci. Rep. Whales. Res. Inst.* **32**, 155-197.

Kielhorn, C. E., Dillaman, R. M., Kinsey, S. T., McLellan, W. A., Gay, D. M., Dearolf, J. L. and Pabst, D. A. (2013). Locomotor muscle profile of a deep (*Kogia breviceps*) versus shallow (*Tursiops truncatus*) diving cetacean. *J. Morphol.* **274**, 663-675.

Kohn, T. A., Essén-Gustavsson, B. and Myburgh, K. H. (2007). Do skeletal muscle phenotypic characteristics of Xhosa and Caucasian endurance runners differ when matched for training and racing distances? *J. Appl. Physiol.* **103**, 932-940.

Kohn, T. A., Burroughs, R., Hartman, M. J. and Noakes, T. D. (2011a). Fiber type and metabolic characteristics of lion (*Panthera leo*), caracal (*Caracal caracal*) and human skeletal muscle. *Comp. Biochem. Physiol. A Mol. Integr. Physiol.* **159**, 125-133.

Kohn, T. A., Curry, J. W. and Noakes, T. D. (2011b). Black wildebeest skeletal muscle exhibits high oxidative capacity and a high proportion of type IIx fibres. *J. Exp. Biol.* **214**, 4041-4047.

Kooyman, G. L., Wahrenbrock, E. A., Castellini, M. A., Davis, R. W. and Sinnett, E. E. (1980). Aerobic and anaerobic metabolism during voluntary diving in Weddell seals: evidence of preferred pathways from blood chemistry and behavior. *J. Comp. Physiol. B* **138**, 335-346.

Lefaucheur, L., Milan, D., Ecolan, P. and Le Callennec, C. (2004). Myosin heavy chain composition of different skeletal muscles in Large White and Meishan pigs. *J. Anim. Sci.* **82**, 1931-1941.

Li, X., Higashida, K., Kawamura, T. and Higuchi, M. (2016). Alternate-day high-fat diet induces an increase in mitochondrial enzyme activities and protein content in rat skeletal muscle. *Nutrients* **8**, 203.

Lopez-Rivero, J. L., Serrano, A. L., Diz, A. M. and Galisteo, A. M. (1992). Variability of muscle fibre composition and fibre size in the horse gluteus medius: an enzyme-histochemical and morphometric study. *J. Anat.* **181**, 1-10.

Lovell, D. K. and Rose, R. J. (1991). Changes in skeletal muscle composition in response to interval and high intensity training. In *Equine Exercise Physiology 3* (ed. S. G. B. Persson, A. Lindholm and L. B. Jeffcott), pp. 215-222. Uppsala, Sweden: ICEEP Publications.

Lui, M. A., Mahalingam, S., Patel, P., Connaty, A. D., Ivy, C. M., Cheviron, Z. A., Storz, J. F., McClelland, G. B. and Scott, G. R. (2015). High-altitude ancestry and hypoxia acclimation have distinct effects on exercise capacity and muscle phenotype in deer mice. *Am. J. Physiol. Regul. Integr. Comp. Physiol.* **308**, R779-R791.

MacDougall, J. D., Hicks, A. L., MacDonald, J. R., McKelvie, R. S., Green, H. J. and Smith, K. M. (1998). Muscle performance and enzymatic adaptations to sprint interval training. *J. Appl. Physiol.* **84**, 2138-2142.

Martin, T. P., Vailas, A. C., Durivage, J. B., Edgerton, V. R. and Castleman, K. R. (1985). Quantitative histochemical determination of muscle enzymes: biochemical verification. *J. Histochem. Cytochem.* **33**, 1053-1059.

Marx, F. G., Lambert, O. and Uhen, M. D. (2016). Cetaceans, past and present. In *Cetacean Paleobiology* (ed. M. J. Benton), pp. 1-18. The Atrium, UK: John Wiley & Sons, Ltd.

Noren, S. R. and Williams, T. M. (2000). Body size and skeletal muscle myoglobin of cetaceans: adaptations for maximizing dive duration. *Comp. Biochem. Physiol. A Mol. Integr. Physiol.* **126**, 181-191.

Nwoye, L., Mommaerts, W. F., Simpson, D. R., Seraydarian, K. and Marusich, M. (1982). Evidence for a direct action of thyroid hormone in specifying muscle properties. *Am. J. Physiol.* **242**, R401-R408.

Orton, L. S. and Brodie, P. F. (1987). Engulfing mechanics of fin whales. *Can. J. Zool.* **65**, 2898-2907.

Pabst, D. A. (2000). To bend a dolphin: convergence of force transmission designs in cetaceans and scombrid fishes. *Am. Zool.* **40**, 146-155.

Polasek, L. K. and Davis, R. W. (2001). Heterogeneity of myoglobin distribution in the locomotory muscles of five cetacean species. *J. Exp. Biol.* **204**, 209-215.

Polasek, L. K., Dickson, K. A. and Davis, R. W. (2006). Metabolic indicators in the skeletal muscles of harbor seals (*Phoca vitulina*). *Am. J. Physiol. Regul. Integr. Comp. Physiol.* **290**, R1720-R1727.

Potvin, J., Goldbogen, J. A. and Shadwick, R. E. (2009). Passive versus active engulfment: verdict from trajectory simulations of lunge-feeding fin whales *Balaenoptera physalus*. *J. R Soc. Interface* **6**, 1005-1025.

Potvin, J., Goldbogen, J. A. and Shadwick, R. E. (2012). Metabolic expenditures of lunge feeding rorquals across scale: implications for the evolution of filter feeding and the limits to maximum body size. *PLoS ONE* **7**, e44854.

Quiroz-Rothe, E. and Rivero, J.-L. L. (2001). Co-ordinated expression of contractile and non-contractile features of control equine muscle fibre types characterised by immunostaining of myosin heavy chains. *Histochem. Cell Biol.* **116**, 299-312.

Quiroz-Rothe, E. and Rivero, J.-L. L. (2004). Coordinated expression of myosin heavy chains, metabolic enzymes, and morphological features of porcine skeletal muscle fiber types. *Microsc. Res. Tech.* **65**, 43-61.

Reed, J. Z., Butler, P. J. and Fedak, M. A. (1994). The metabolic characteristics of the locomotory muscles of grey seals (*Halichoerus grypus*), harbour seals (*Phoca vitulina*) and Antarctic fur seals (*Arctocephalus gazella*). *J. Exp. Biol.* **194**, 33-46.

Reynafarje, B. (1963). Simplified method for the determination of myoglobin. *J. Lab. Clin. Med.* **61**, 138-145.

Rivero, J.-L. L., Ruz, A., Martí-Korff, S., Estepa, J.-C., Aguilera-Tejero, E., Werkman, J., Sobotta, M. and Lindner, A. (2007). Effects of intensity and duration of exercise on muscular responses to training of thoroughbred racehorses. *J. Appl. Physiol.* **102**, 1871-1882.

Rivero, J.-L. L., Serrano, A. L., Barrey, E., Valette, J. P. and Jouglin, M. (1999). Analysis of myosin heavy chains at the protein level in horse skeletal muscle. *J. Muscle Res. Cell Motil.* **20**, 211-221.

Rivero, J.-L. L., Serrano, A. L. and Henckel, P. (1995). Activities of selected aerobic and anaerobic enzymes in the gluteus medius muscle of endurance horses with different performance records. *Vet. Rec.* **137**, 187-192.

Rivero, J.-L. L., Talmadge, R. J. and Edgerton, V. R. (1996a). Correlation between myofibrillar ATPase activity and myosin heavy chain composition in equine skeletal muscle and the influence of training. *Anat. Rec.* **246**, 195-207.

Rivero, J.-L. L., Talmadge, R. J. and Edgerton, V. R. (1996b). Myosin heavy chain isoforms in adult equine skeletal muscle: an immunohistochemical and electrophoretic study. *Anat. Rec.* **246**, 185-194.

Rivero, J.-L. L., Talmadge, R. J. and Edgerton, V. R. (1997). A sensitive electrophoretic method for the quantification of myosin heavy chain isoforms in horse skeletal muscle: histochemical and immunocytochemical verifications. *Electrophoresis* **18**, 1967-1972.

Rivero, J.-L. L., Talmadge, R. J. and Edgerton, V. R. (1998). Fibre size and metabolic properties of myosin heavy chain-based fibre types in rat skeletal muscle. *J. Muscle Res. Cell Motil.* **19**, 733-742.

Rossini, K., Rizzi, C., Sandri, M., Bruson, A. and Carraro, U. (1995). High-resolution sodium dodecyl sulfate-polyacrylamide gel electrophoresis and immunochemical identification of the 2X and embryonic myosin heavy chains in complex mixtures of isomyosins. *Electrophoresis* **16**, 101-104.

Schiaffino, S. and Reggiani, C. (2011). Fiber types in mammalian skeletal muscles. *Physiol. Rev.* **91**, 1447-1531.

Schiaffino, S., Gorza, L., Sartore, S., Saggin, L., Ausoni, S., Vianello, M., Gundersen, K. and Lømo, T. (1989). Three myosin heavy chain isoforms in type 2 skeletal muscle fibres. *J. Muscle Res. Cell Motil.* **10**, 197-205.

Shadwick, R. E., Goldbogen, J. A., Potvin, J., Pyenson, N. D. and Vogl, A. W. (2013). Novel muscle and connective tissue design enables high extensibility and controls engulfment volume in lunge-feeding rorqual whales. *J. Exp. Biol.* **216**, 2691-2701.

Southern, W. M., Nichenko, A. S., Shill, D. D., Spencer, C. C., Jenkins, N. T., McCully, K. K. and Call, J. A. (2017). Skeletal muscle metabolic adaptations to endurance exercise training are attainable in mice with simvastatin treatment. *PLoS ONE* **12**, e0172551.

Suzuki, A., Tsuchiya, T., Takahasgi, Y. and Tamate, H. (1983). Histochemical properties of myofibers in longissimus muscle of common dolphins (*Delphinus delphis*). *Acta Histochem. Cytochem.* **16**, 223-231.

Talmadge, R. J. and Roy, R. R. (1993). Electrophoretic separation of rat skeletal muscle myosin heavy-chain isoforms. *J. Appl. Physiol.* **75**, 2337-2340.

Tomilin, A. G. (1957). *Mammals of the USS. Royal and Adjacent Countries*, Vol. IX. Cetacea. Moscow, Russia: Nauk USSR.

Tyack, P. L., Johnson, M., Soto, N. A., Sturlese, A. and Madsen, P. T. (2006). Extreme diving of beaked whales. *J. Exp. Biol.* **209**, 4238-4253.

Velten, B. P., Dillaman, R. M., Kinsey, S. T., McLellan, W. A. and Pabst, D. A. (2013). Novel locomotor muscle design in extreme deep-diving whales. *J. Exp. Biol.* **216**, 1862-1871.

Wang, Z. M., O'Connor, T. P., Heshka, S. and Heymsfield, S. B. (2001). The reconstruction of Kleiber's law at the organ-tissue level. *J. Nutr.* **131**, 2967-2970.

Watkins, W. A., Sigurjónsson, J., Wartzok, D., Maiefski, R. R., Howey, P. W. and Daher, M. A. (1996). Fin whale tracked by satellite off Iceland. *Mar. Mamm. Sci.* **12**, 564-569.

Watson, R. R., Miller, T. A. and Davis, R. W. (2003). Immunohistochemical fiber typing of harbor seal skeletal muscle. *J. Exp. Biol.* **206**, 4105-4111.

Watson, R. R., Kanatous, S. B., Cowan, D. F., Wen, J. W., Han, V. C. and Davis, R. W. (2007). Volume density and distribution of mitochondria in harbor seal (*Phoca vitulina*) skeletal muscle. *J. Comp. Physiol. B* **177**, 89-98.

Weibel, E. R. and Hoppeler, H. (2005). Exercise-induced maximal metabolic rate scales with muscle aerobic capacity. *J. Exp. Biol.* **208**, 1635-1644.

Williams, T. M. and Noren, S. R. (2011). Extreme physiological adaptations as predictors of climate-change sensitivity in the narwhal, *Monodon monoceros*. *Mar. Mammal Sci.* **27**, 334-349.

Williams, T. M., Dobson, G. P., Mathieu-Costello, O., Morsbach, D., Worley, M. B. and Phillips, J. A. (1997). Skeletal muscle histology and biochemistry of an elite sprinter, the African cheetah. *J. Comp. Physiol. B* **167**, 527-535.

Yamada, T., Furuichi, Y., Takakura, H., Hashimoto, T., Hanai, Y., Jue, T. and Masuda, K. (2013). Interaction between myoglobin and mitochondria in rat skeletal muscle. *J. Appl. Physiol.* **114**, 490-497.

Yoshida, Y., Holloway, G. P., Ljubicic, V., Hatta, H., Spriet, L. L., Hood, D. A. and Bonen, A. (2007). Negligible direct lactate oxidation in subsarcolemmal and intermyofibrillar mitochondria obtained from red and white rat skeletal muscle. *J. Physiol.* **582**, 1317-1335.

Zomeño, C., Blasco, A. and Hernández, P. (2010). Influence of genetic line on lipid metabolism traits of rabbit muscle. *J. Anim. Sci.* **88**, 3419-3427.